ISET Journal of Earthquake Technology, Paper No. 381, Vol. 35, No. 4, December 1998, pp. 167-184

SEISMIC DESIGN, ANALYSIS AND EXPERIMENT OF A MULTI-STORY VISCOELASTICALLY DAMPED STEEL FRAME

Christopher Higgins* and Kazuhiko Kasai**

*Assistant Professor, Department of Civil Engineering,
Clarkson University, W. J. Rowley Laboratories, Box 5710, Potsdam, NY 13699
**Professor, Tokyo Institute of Technology, Structural Engineering Research Center,
Nagatsuta, Midori-Ku, Yokohama 226-8503, Japan

ABSTRACT

This paper describes the design, analysis, and laboratory tests of a prototype viscoelastically (VE-) damped steel frame building. A design approach is presented for a 10-story building with specified high-performance criteria including elastic member behavior and small drift for the 500 year return period design earthquake. Nonlinear time-history analyses with a fractional derivative model for the VE-dampers were conducted and are compared with specified design goals. A unique methodology was developed to test the full-scale, lower 3-story portion of the prototype VE-structure which relies on time-history analyses to determine the displacement for the laboratory test frame. The testing methodology is presented and experimentally observed VE-frame response is discussed. Experimental results are described including overall frame response, local member response, and damper-member interaction.

KEYWORDS: Viscoelastic Damping, Design, Analysis, Experiment

INTRODUCTION AND BACKGROUND

The application of viscoelastic dampers (VE-) to building structures has recently attracted the interest of the earthquake engineering community due to the dramatic changes in dynamic structural response resulting from the additional stiffness and damping provided by VE-dampers (Aiken and Kelly 1991, Chang et al. 1991, Kasai and Fu 1995). VE-dampers show significant potential for providing economic structures, which can behave elastically and develop small drifts even when subjected to a major earthquake, thereby protecting both structural and non-structural components. In order to validate VE-frame analysis and design methods, a full-scale three-story portion of a steel frame with VE-dampers has been tested under simulated seismic loading. This paper presents a design methodology for a multi-story VE-frame, time-history analysis results, and full-scale and real-time experimental response of the VE-frame to simulated earthquake ground motions. The key response parameters are correlated among design, analysis, and experiments.

SEISMIC FORCE AND DRIFT REQUIREMENTS

To permit assessment of the seismic behavior for a VE-damped steel frame, a prototype 10-story steel frame building was designed. The prototype structure was chosen to be an ordinary office building located in San Francisco, California on very dense soil. A building layout was established in an attempt to reflect an actual structure and to meet additional requirements for experimental testing such as force, displacement, and loading frequency capabilities of available hydraulic actuators as well as space and hold-down locations in the testing laboratory. The plan and elevation of the selected prototype VE-building are shown in Figure 1. Building response was considered for the east-west direction only and all VE-frames in the east-west direction were identical. The additional framing members only support gravity loads and did not contribute to lateral force resistance.

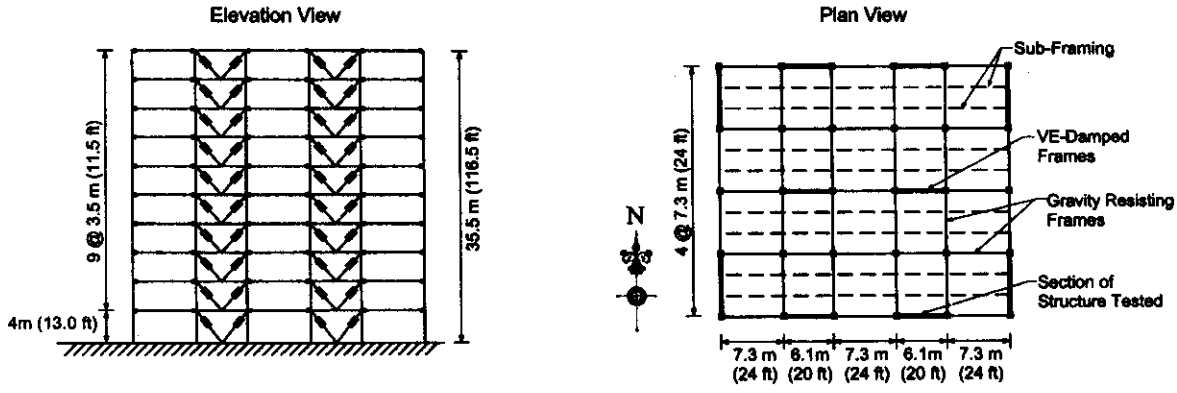

Fig. 1 Plan and elevation view of multi-story prototype viscoelastically damped steel frame.

The frame was designed to satisfy two criteria:

- The structure should remain elastic against the design based earthquake (DBE) at the reference temperature of 24 °C.
- The building should protect non-structural components for the DBE by limiting the drift to 0.0075 radians at 24 °C.

While the selected drift criteria would not preclude damage, it does greatly enhance the damage resistance of the prototype building and contents when subjected to a major earthquake as compared to the typical NEHRP drift limits of 1 % to 1.5 %. To economically achieve this level of seismic performance, the structure requires some type of supplemental damping device. For this study, VE-dampers were considered.

DESIGN FORCES

Design of the VE-frame was performed using a NEHRP (1994) based equivalent static force design procedure developed by Kasai and Fu (1995). The procedure consistently uses elastic static analysis and for the first time employs various design techniques: to obtain the dynamic properties of the VE-frame such as vibration period and damping ratio; to estimate the high damping global responses like displacement, acceleration, and force; and to estimate local responses such as peak forces in the dampers, connections, beams, and columns. It differs from Chang et al.'s technique (1995) which uses eigenvalue analysis of the VE-frame as well as assumes the same loss factor of the damper-brace components through the height of the building. The design base shear spectrum from the NEHRP provisions (1994) is:

$$V_{DBE} = \frac{1.2C_v}{T^{2/3}} W \le 2.5C_a W \tag{1}$$

where V_{DBE} is the base shear for an elastic building subjected to the DBE, T is the building period, W is the total weight of the building, C_v is a seismic coefficient which depends on the soil type and effective peak velocity-related acceleration ($A_v = 0.4$ for selected site), and C_a is a seismic coefficient which depends on the soil type and effective peak acceleration ($A_a = 0.4$ for selected site). The prototype frame is located on a site with very dense soil corresponding to NEHRP soil profile B/C, which results in $C_v = 0.48$ and $C_a = 0.40$ respectively. The required NEHRP yield base shear strength is:

$$V_{yield} = \frac{V_{DBE}}{R} \tag{2}$$

where R is a strength reduction factor which depends on the type of framing used by the structure. Equation (2) anticipates yielding and ductility of the frame when subjected to the DBE. However, we will consider maintaining elastic response of the structural members even against the DBE (i.e., $R=1$). In such a case, a conventional structure would require a large V_{yield} and consequently large members and connections. The VE-frame uses VE-dampers to reduce the earthquake forces by providing high damping. To include the beneficial effects of higher damping, the yield base shear strength becomes:

$$V_{yield} = D_\xi V_{DBE} \tag{3}$$

where D_ξ is a parameter which indicates the effect of the higher damping in reducing the DBE base shear. The damping effect parameter is defined (Kasai and Fu, 1995, Kasai et al. 1998) as:

$$D_\xi = \frac{1.5}{\sqrt{1+25\xi}} \tag{4}$$

where ξ is the frame damping ratio. Note the NEHRP spectrum (Equation (1)) uses a ξ of 5 % for which $D_\xi = 1.0$. The design pseudo-acceleration spectrum $S_{pa}(T,\xi)$ for a highly damped VE-frame is:

$$S_{pa}(T,\xi) = D_\xi \frac{1.2C_v}{T^{2/3}} \le D_\xi 2.5C_a \tag{5}$$

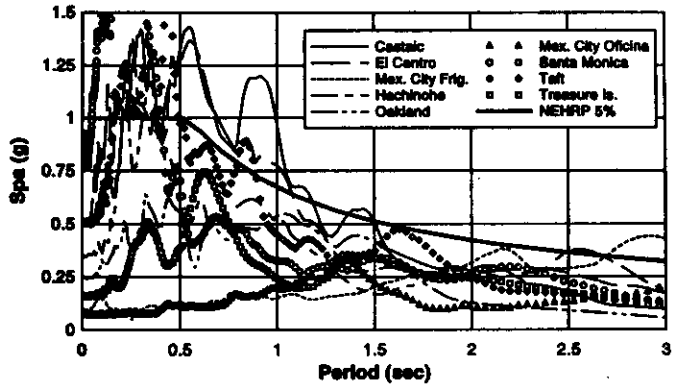

Fig. 2 Spectral acceleration for design and selected earthquakes ξ=5%.

The design pseudo-acceleration spectrum is shown in Figures 2 and 3 for damping ratios of 5 % and 30 % respectively. As seen in these figures, the DBE acceleration decreases as the damping ratio increases, resulting in lower required base shear. The design displacement spectrum $S_d(T,\xi)$ is:

$$S_d(T,\xi) = \frac{T^2}{4\pi^2} D_\xi \frac{1.2C_v}{T^{2/3}} \le \frac{T^2}{4\pi^2} D_\xi 2.5C_a \tag{6}$$

The design displacement spectrum is shown in Figures 4 and 5 for damping ratios of 5 % and 30 % respectively. Here also, higher damping results in reduced building deformation.

Many different combinations of building period and damping ratio are possible for the prototype frame. The building period was initially estimated from the NEHRP approximate formula for the fundamental period (NEHRP 1994) as:

$$T_a = C_T h_n^{3/4} \tag{7}$$

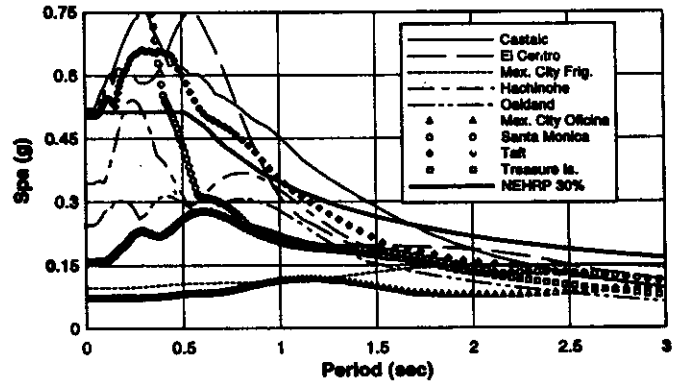

Fig. 3 Spectral acceleration for design and selected earthquakes ξ=30%.

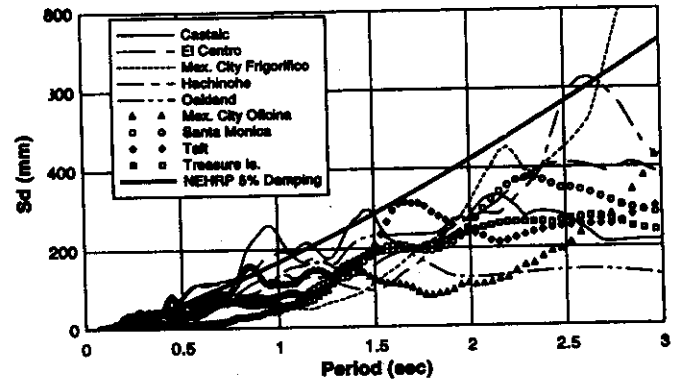

Fig. 4 Spectral displacement for design and selected earthquakes ξ=5%.

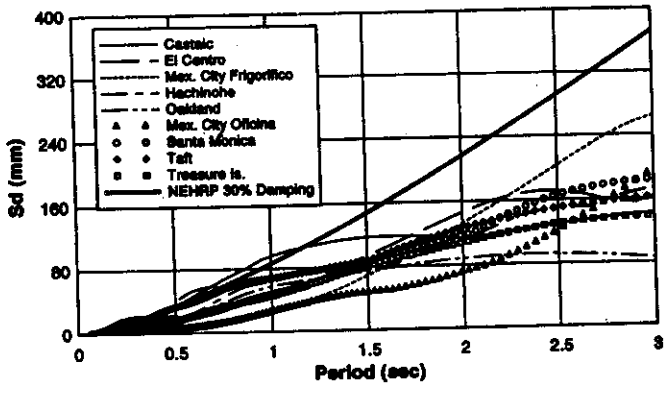

Fig. 5 Spectral displacement for design and selected earthquakes ξ=30%.

where C_T is a coefficient which is related to the framing system, and h_n is the height of the building in feet. $C_T = 0.03$, specified for an eccentrically braced frame, is used for the VE-frame with stiff dampers. The building period estimate from Equation (7) is typically lower than the actual period, which is generally conservative from the perspective of strength requirement. However, Equation (7) would result

in an unconservative estimate of lateral drift. For the prototype frame, T_a was 1.06 sec (Equation (7)) for which the required $S_{pa}(1.06,\xi) = 0.553$ g, 0.443 g, 0.338 g, and 0.284 g for ξ = 5 %, 10 %, 20 %, and 30 %. A target damping ratio of 30 % was selected to minimize the DBE base shear. From Equation (6), the actual building period T must be below 1.17, 1.38, 1.69, and 1.94 sec for ξ = 5 %, 10 %, 20 %, and 30 % to keep the frame drift below 0.0075 radians. Limits on actual building period were estimated by noting that when the fundamental mode shape of a multi-degree of freedom (MDOF) system is a straight-line, the maximum roof displacement is 3/2 times $S_d(T,\xi)$. Highly damped VE-structures tend to exhibit straight-line fundamental mode shapes (Kasai et al. 1993). For the target damping ratio of 30 %, the actual building period must be below 1.94 sec to achieve the desired drift performance.

Dead load on the floors was 3.7 kPa (78 psf) and curtain wall dead load was 0.7 kPa (15 psf). The total dead weight of the building was 40.65 MN (9139.2 kips). Traditionally, building code specifications compute the required base shear as $S_{pa}M_{tot}$. For the MDOF VE-frame, which exhibits a straight-line fundamental mode shape, the theoretical base shear is $S_{pa}M_{tot}/1.33$. Thus, the theoretical required yield strength for the seismic prototype frame is:

$$V_{yield} = \frac{S_{pa}(T = T_a = 1.06, \xi = 30\%)M_{tot}}{1.33} \tag{8}$$

From Equation (8), the required yield strength was 8670 kN (1949.2 kips) for the prototype frame. This total base shear was shared equally among the six VE-frames in the east-west direction (Figure 1). The total base shear was distributed vertically to each story level according to the NEHRP formula:

$$F_i = V_{yield}\frac{w_i h_i^k}{\sum_{i=1}^{N} w_i h_i^k} \tag{9}$$

where w_i is the portion of the gravity load at level i (kN or kips), h_i is the height from the base to level i (m or ft), k is a coefficient which is related to the building period, and N is the number of stories. The coefficient k is 1.0 for a building with a period of 0.5 sec or less, 2.0 for a building with a period of 2.5 sec or more, and is determined by interpolation for a building with a period between 0.5 and 2.5 sec. The design lateral forces at each story level and computed over-turning moment applied to each of the six VE-frames in the prototype building are shown in Table 1.

Table 1: Story Lateral Forces, Cumulative Shear Forces and Overturning Moments for Design using NEHRP Approximate Period

Story	Height		Floor Weight #		Lateral Force		Cummulative Shear		Overturning Moment	
Level	(m)	(ft)	(kN)	(kips)	(kN)	(kips)	(kN)	(kips)	(kN-m)	(kip-ft)
1	4.0	13.0	677.5	152.3	4.9	1.1	1445.0	324.9	473045	348853
2	7.5	24.5	677.5	152.3	14.7	3.3	1437.6	323.2	404324	298174
3	11.0	36.0	677.5	152.3	28.9	6.5	1415.1	318.1	343845	253573
4	14.5	47.5	677.5	152.3	46.9	10.5	1371.0	308.2	284311	209669
5	18.0	59.0	677.5	152.3	68.5	15.4	1299.4	292.1	226632	167133
6	21.5	70.5	677.5	152.3	93.6	21.0	1194.7	268.6	171967	126819
7	25.0	82.0	677.5	152.3	121.9	27.4	1051.8	236.5	121705	89753
8	28.5	93.5	677.5	152.3	153.4	34.5	865.6	194.6	77456	57121
9	32.0	105.0	677.5	152.3	187.9	42.2	631.3	141.9	41042	30267
10	35.5	116.5	677.5	152.3	225.3	50.7	344.3	77.4	14483	10681

Contribution assigned to each of the six VE-frames.

DESIGN OF VISCOELASTIC FRAME

In order to size the damper and members, the design force (Equation (9)) must be distributed to these components considering their relative stiffness. Hereby, a ratio between the horizontal stiffness of the damper K'_d and frame K_f is considered. The role of K'_d/K_f on the equivalent damping ratio ξ for a single degree of freedom (SDOF) system is shown in Figure 6 for an assumed $\eta_d = 1.32$ at the reference temperature of 24 °C, a loading frequency of 0.5 Hz, and strain of 50 %. From Figure 6, very high ξ of 33 % is desired, for which the damper to frame stiffness ratio $K'_d/K_f = 3$ in the lower three stories and brace to frame stiffness ratio $K_b/K_f \geq 20$ were required. A stiff damper was desired because it attracts force. A stiff brace was also desired because it permits the force attracted by the damper to be dissipated by enabling deformation to take place in the VE-material instead of in elastic deformation of the brace. Note also from Figure 6 that ξ is relatively stable even as K'_d/K_f varies due to temperature changes in the VE-material. Thus, one way to control temperature sensitivity of the damping ratio is to provide a stiff damper and a stiff brace relative to the frame stiffness without dampers. Note also that in Figure 6, control of the damping ratio is also possible when the brace is soft, however such a case results in much lower damping and is recommended only when relatively low supplemental damping is required.

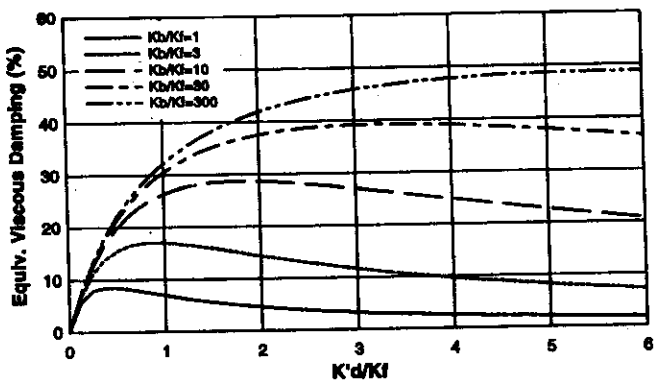

Fig. 6 Equivalent damping for SDOF system with various frame, damper and brace stiffness ratios

In the present study, the dampers at each story level were proportioned based on the above stiffness ratio. Although the damping ratio of a MDOF VE-frame is typically less than that of a SDOF system, due to chord drift (caused by column axial deformation) which does not promote energy dissipation in the VE-dampers, the final damping ratio for the MDOF VE-frame should be close to the target of 30 %.

The portal method, modified to consider effects of the viscous force created by the VE-dampers, was used to obtain the maximum member forces from the computed lateral loads (Equation (9)) and the required stiffness ratios. The method combines the force in-phase with the frame drift (elastic force) and that 90° out-of-phase (viscous force) in a vectorial manner to compute the maximum member forces (Kasai and Fu 1995, Fu and Kasai 1998). In addition to seismic forces, gravity forces were included using the AISC LRFD (1993) load combination $1.2DL + 0.5LL \pm E$, where DL is the dead load, LL is the live load, and E is the earthquake lateral load. Live load on the floors was 2.4 kPa (50 psf) and live load reduction factors were used for beams and columns as permitted by ASCE 7-95.

Beams and columns were designed using A572 grade 50 steel and connection pieces were designed using A36 steel. Members were sized based on the computed maximum forces described above. Beams

and columns were designed considering the combined axial force and moment interaction using the AISC LRFD (1993) interaction equations:

$$\text{for } \frac{P_u}{\phi_c P_n} \geq 0.2 \qquad \frac{P_u}{\phi_c P_n} + \frac{8}{9}\left(\frac{M_u}{\phi_b M_n}\right) \leq 1.0 \tag{10a}$$

$$\text{for } \frac{P_u}{\phi_c P_n} < 0.2 \qquad \frac{P_u}{2\phi_c P_n} + \frac{M_u}{\phi_b M_n} \leq 1.0 \tag{10b}$$

where P_u and M_u are the maximum axial force and moment on the member from the applied loads, and P_n and M_n are the nominal axial force and moment capacities of the member, $\phi_c = 0.85$ is the axial force strength reduction factor and $\phi_b = 0.9$ is moment strength reduction factor. Maximum axial load and moment occur at different instances of time due to a viscous force contribution from the VE-dampers (Kasai and Fu 1995, Fu and Kasai 1998), however for conservative design, peak forces are assumed to occur simultaneously. This point will be discussed further, using the experimental results.

Square tube sections corresponding to A500 Grade B ($F_y = 317$ MPa (46 ksi)) were used for the braces, which attach the VE-dampers to the frame. Brace size for the added component was determined using the computed axial forces from the portal analysis described previously. For additional conservatism, the axial force in the brace was amplified by a factor of 1.5 to prevent possible brace buckling (Kasai and Popov 1986). Effective length factors of $k_x = k_y = 0.8$ and strength reduction factor $\phi = 0.85$ were used for design of the braces.

PERIOD AND DAMPING ESTIMATE FROM ELASTIC STATIC ANALYSIS

With the member sizes obtained above, elastic static analysis was performed for the frame without dampers. This analysis was performed to determine the shear stiffness of the frame K_f. Beam-column and column base connections were assumed rigid and center-line frame dimensions were used for the model. Subsequent laboratory tests of the bare steel frame indicated the beam-column connections behaved as rigid connections (Kasai and Higgins 1997). To isolate the frame shear stiffness, axial deformations in the columns were suppressed by artificially increasing the cross sectional area. Suppression of column axial deformation was done for this analysis only. Lateral forces determined previously were used to load the unbraced frame model. The computed frame shear stiffness was $\approx$3 kN/mm (17.2 kips/in) in a typical lower story. Using the target ratio $K'_d/K_f = 3$ at each story level, the required damper stiffness K'_d was determined. Similarly, the brace stiffness K_b was determined for the brace sizes selected in the previous section assuming center-line dimensions for the member and axial area of the tube only. The stiffness K'_a of the combined VE-damper and brace assembly, termed 'added component', was computed assuming a loss factor $\eta_d = 1.32$ (for the required vibration period of 1.94 sec, as described earlier) and using K'_d and K_b at each story stiffness from:

$$K'_a = \frac{K_b K'_d}{(K_b/\Gamma) + K'_d} \tag{11}$$

where

$$\Gamma = 1 + \frac{\eta_d^2}{(1 + K_b/K'_d)} \tag{12}$$

Following analysis of the unbraced frame, an analytical model of the VE-frame was developed. The added components were modeled with linear elastic truss elements with horizontal stiffness K'_a. The fundamental building period T was calculated using Rayleigh's method as:

$$T = 2\pi \sqrt{\frac{\sum_{i=1}^{N} W_i \Delta_i^2}{g \sum_{i=1}^{N} F_i \Delta_i}} \tag{13}$$

where W_i are the story weights, Δ_i are the story lateral displacements, and F_i are the story forces (Equation (9)) at the i-th story respectively, and g is the gravitational acceleration. The computed period (Equation (13)) was 2.0 sec, which is larger than the $T_a = 1.06$ sec used in preliminary design. The period is also very close to the required period of 1.94 sec for drift control at $\xi = 30\,\%$.

Equivalent viscous damping ξ_{tot} for the VE-frame was calculated using an energy approach and static analysis (Kasai et al. 1993, Fu and Kasai 1998) as:

$$\xi_{tot} = \xi_o + \frac{\sum \eta_a F_a u_a}{2 \sum_{i=1}^{N} F_i \Delta_i} \tag{14}$$

where $\sum_{i=1}^{N} F_i \Delta_i$ is the total work done by external lateral forces where Δ_i and F_i are defined previously, $\sum \eta_a F_a u_a$ is the total energy dissipated by the VE-dampers where u_a and F_a are the deformation and force of the added component respectively, ξ_o is the unbraced frame damping ratio (2 %) and N is the number of stories. The computed damping ratio ξ_{tot} was 30.2 %, which is very close to the 30 % assumed during initial design.

VISCOELASTIC DAMPER DESIGN

The VE-damper was designed based on the structural deformation computed from static analysis of the vertically distributed design base shear. Thickness of the VE-layer $h = 16\,\text{mm}$ (0.625 in) was selected so as to limit the maximum shear strain γ to below 100 %. An average γ of 0.7 times the maximum shear strain was considered as an average VE-material strain during a random earthquake event. For the selected damper thickness $h = 16\,\text{mm}$ (0.625 in), reference temperature of 24°C, VE-frame building period of 2.0 sec, and average strain of 70 %, and storage modulus $G' = 786$ kPa (114 psi) determined from the manufacturer's data, the required damper area A was determined by:

$$A = \frac{\left(K'_d / \cos^2 \theta\right) h}{G'} \tag{15}$$

to provide the required damper stiffness, where θ is the inclination angle of the damper. The required area of VE-material was 805,210 mm^2 (1248 in^2) for each damper. The four faces of the steel tube permit a large amount of VE-material to be placed in a relatively small volume of space.

FINAL DESIGN OF TEST SPECIMEN

After completing the design steps in the previous sections, the initial frame design was refined to include lateral forces for the actual building period as well as actual damper stiffness and loss factors.

This was done to provide frame member sizes which were as small as possible to permit applied laboratory forces and displacements to be within testing capabilities and to enable application of significant stress in members during the tests. The final member selection was performed iteratively following the previously described design procedure. The final fundamental period was 2.0 sec which results in $S_{pa}(2.0,\xi)$ = 0.186 g for ξ = 30.2 % which was the final damping ratio. The required base shear for the prototype structure was 5675.4 kN (1275.6 kips) which is less than required base shear using the NEHRP approximate building period. Using the portal method with the lateral forces corresponding to the 2.0 sec building period, the maximum member forces were computed as shown in Table 2. Final member and brace sizes are shown in Table 3. The final design met the strength requirement of elastic performance and the drift requirement less than 0.0075 radians at the reference temperature for the DBE. Later time-history analysis of the frame subjected to selected earthquake ground motions indicated the frame drift requirement was met and the frame members behaved elastically.

Table 2: Frame Member Forces from Modified Portal Method

Story Level	Beam Axial Force		Beam Moment		Column Axial Force		Column Moment		Column Shear Force		Damper Axial Force	
	(kN)	(kips)	(kN-m)	(kip-ft)	(kN)	(kips)	(kN-m)	(kip-ft)	(kN)	(kips)	(kN)	(kips)
1	1028.6	231	463.4	342	6673.0	1500	234.3	173	118.2	27	1567.6	352
2	1023.3	230	432.1	319	5785.3	1301	206.2	152	117.6	26	1559.5	351
3	1007.3	226	422.6	312	4948.9	1113	203.0	150	115.8	26	1535.1	345
4	975.9	219	406.0	299	4125.4	927	196.6	145	112.2	25	1487.3	334
5	925.0	208	380.7	281	3326.0	748	186.4	137	106.3	24	1409.6	317
6	850.4	191	345.2	255	2564.6	577	171.4	126	97.8	22	1296.1	291
7	748.7	168	298.0	220	1858.1	418	150.9	111	86.1	19	1141.0	257
8	616.1	139	237.6	175	1225.5	276	124.1	92	70.8	16	939.0	211
9	449.4	101	162.9	120	688.7	155	90.5	67	51.7	12	684.8	154
10	245.1	55	72.3	53	271.5	61	49.4	36	28.2	6	373.5	84

Table 3: Final Selection of Member Sizes for VE-Frame

Story Level	Beam Member	Column Member	Brace Member
1	W18x50	W14x159	TS8x8x1/2
2	W18x40	W14x159	TS8x8x1/2
3	W18x40	W14x159	TS8x8x1/2
4	W18x40	W14x145	TS8x8x3/8
5	W18x35	W14x145	TS8x8x3/8
6	W18x35	W14x145	TS8x8x3/8
7	W16x31	W14x82	TS8x8x1/4
8	W16x31	W14x82	TS8x8x1/4
9	W10x19	W14x48	TS7x7x3/16
10	W10x19	W14x48	TS7x7x3/16

After the seismic design was complete, the frame was checked for strength against the code prescribed wind forces in ASCE 7-95. The design wind speed was 38 m/s (85 mph) for San Francisco, California. To compute the strength of the frame for wind forces, the AISC LRFD (1993) load combination was employed. The contribution of the VE-dampers was conservatively neglected for wind analyses (Higgins and Kasai 1998) and the VE-frames were modeled as unbraced frames. Member forces and frame drifts were evaluated from static analysis of the unbraced frames subjected to the code wind forces. The unbraced frames exhibited sufficient strength and stiffness for the code prescribed wind

forces and gravity loads, including second order effects. Computed frame drifts, including second-order effects, were below 1/500 for short-term effects (ASCE 7-95).

ANALYSIS OF VISCOELASTIC FRAME

Following design, nonlinear time-history analyses were performed of the prototype 10-story VE-frame. Nine different earthquake ground motions were investigated and salient characteristics are presented in Table 4. The selected earthquake records reflect many different characteristics including duration, intensity, frequency content, and soil conditions. An additional criterion for selection required that the records produced structural responses that could be simulated in the laboratory. While the soil conditions varied for the different earthquakes, the highly damped response spectra have the same general trend as the design spectra near the natural frequency of the prototype structure. Acceleration response spectra for the nine records considering equivalent damping ratios of 5 % and 30 % are shown in Figures 2 and 3, respectively. Displacement response spectra for the nine records considering equivalent damping ratios of 5 % and 30 % are shown in Figures 4 and 5, respectively. Three of the records (1.5 x El Centro, 1.5 x Hachinohe, and 2.824 x Taft) are considered design level 2 earthquakes for Japanese seismic design practice (AIJ 1990).

Table 4: Earthquake Records used for Analysis and Experiment

Earthquake	Year	Location	Soil Type	PGA (g)	Duration# (sec)
1.5 x El Centro (N-S)	1940	El Centro, California	Alluvium+	0.52	30
1.5 x Tokachi-Oki (N-S)	1968	Hachinohe, Japan	Deep Cohesionless-	0.34	30
2.824 x Taft (S69E)	1952	Kern County, Califonia	Alluvium+	0.51	30
Oakland (CSMIP 58224 Chan.6) E-W	1989	Loma Prieta, California	Alluvium+	0.25	20
Treasure Island (90)	1989	Loma Prieta, California	Fill+	0.16	15
Castaic Old Ridge Route (360)	1994	Northridge, California	Unknown	0.51	20
Santa Monica City Hall Grounds (90)	1994	Northridge, California	Unknown	0.88	15
Central de Abastos-Frigorifico (E-W)	1985	Mexico City	Soft Clay+	0.10	60
Central de Abastos-Oficina (N-S)	1985	Mexico City	Soft Clay+	0.07	120

Length of record with significant ground shaking.
-[Seed *et al*., 1974] +[Miranda, 1993]

Nonlinear dynamic time history analysis of the prototype VE-frame analytical model was performed using PC-ANSR (Maison 1992). Nonlinear analyses were conducted to assure any nonlinear behavior due to VE-material temperature rise, large amplitude VE-material strain and possible frame member yielding could be accurately captured. The analytical model was subjected to each of the nine earthquake acceleration records applied at the foundation level. Mass of the structure due to dead load only, as well as stiffness and damping of the complete 10-story structure were included in the analysis. Steel frame members were modeled with beam-column elements and the dampers were modeled using a special VE-damper element with an initial VE-material temperature of 24°C as described below.

Nonlinear VE-material behavior was incorporated using a fractional derivative for the stress-strain relationship (Kasai et al., 1993). Parameters used in the constitutive rule were obtained using experimentally determined values for the material storage modulus and loss factor. The material constitutive rule is integrated in a step-by-step analysis procedure to determine the dynamic response of the VE-damper. At each time step, the amount of energy dissipated and the temperature rise are calculated using thermo-mechanics principles and heat transfer theory. Based on the temperature rise and satisfying the VE temperature-frequency equivalence property, parameters for the constitutive rule are updated at each time step. Continuous updating of the parameters results in a nonlinear constitutive rule.

These features have been incorporated into a finite element, which can accurately simulate the nonlinear cyclic behavior of a VE-damper including temperature and excitation frequency effects.

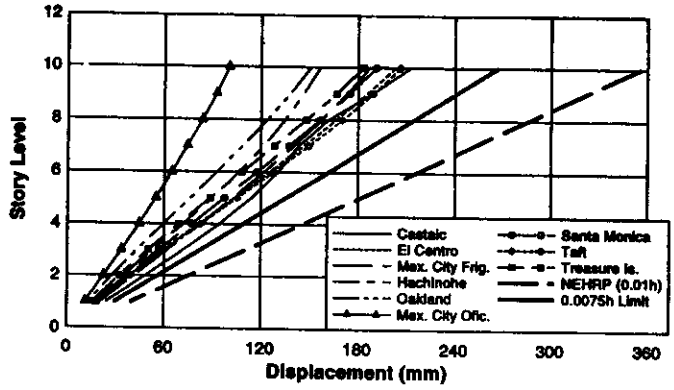

Fig. 7 Peak frame displacements from time-history analyses and design displacement limits

Displacement envelopes produced by each of the nine earthquakes, required design displacements, and the NEHRP displacement limits are shown in Figure 7. The displacement envelopes indicate approximately a straight-line deflected shape for all earthquakes except Northridge-Castaic. Similarly, inter-story drift envelopes for each of the nine earthquakes, specified design drifts, and the NEHRP drift limits are shown in Figure 8. The drifts were all less than the NEHRP 0.01 radians specified drift limit and all but one (Northridge-Castaic) were below the required 0.0075 radians design drift limit. In general, the building exhibited fairly uniform drift for all earthquakes except Northridge-Castaic.

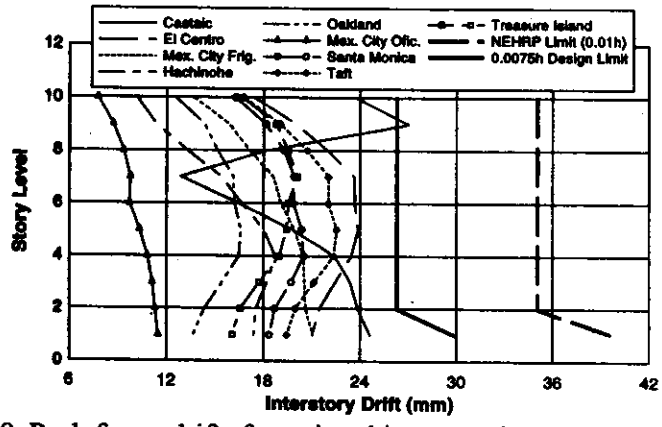

Fig. 8 Peak frame drifts from time-history analyses and design drift limits

Story shear forces were computed by combining the horizontal component of the damper forces and column shear forces to find the maximum at each time-step. It is important to note that the maximum damper force and column shear forces do not occur at the same time and thus simply adding the peak member forces typically results in an over-estimation of the true story shear. Maximum cumulative story shears for each of the nine earthquakes and the design values (Equations (8) and (9)) are shown in Figure 9. As seen in this figure, all but one of the base shears (Northridge-Castaic) were below the design limit. Based on the computed values and due to the conservatism in member design using strength reduction factors of 0.85 and 0.9 (Equations (10a), (10b)), it can be said that the frame members will be elastic against all nine earthquakes. This result was confirmed by comparing computed forces in the frame members with their corresponding yield surfaces.

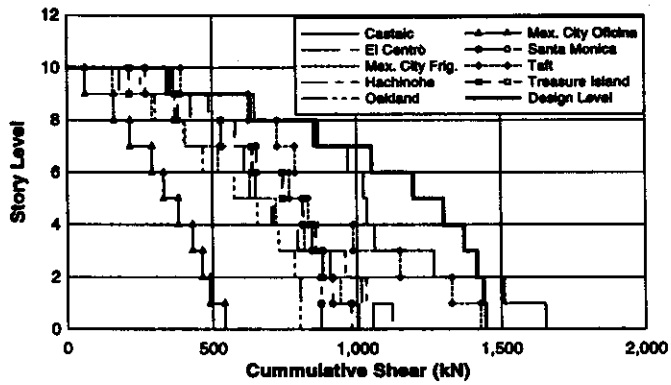

Fig. 9 Peak cumulative shear forces from time-history analyses and design shear forces

The nine earthquakes used for analysis were all below the NEHRP DBE at the 2 sec period of the prototype VE-frame (Figures 2 to 5). Several of the earthquakes would more closely match the specified NEHRP design level earthquake if they were scaled by a factor of approximately 1.3. Peak displacements of the VE-frame subjected to the 1.3 scaled earthquakes can be estimated from Figure 7 assuming linear behavior of the VE-system. Linear scaling is appropriate as the frame members remained elastic and peak VE-material strain amplitudes did not result in significant nonlinear VE-material behavior. This was verified by subsequent nonlinear time-history analysis for the scaled earthquakes. However, if the VE-dampers are not well proportioned or if earthquake induced motions are very large, temperature rise and large strain amplitudes can produce significant nonlinear response. Estimated building drifts for the scaled earthquakes would be less than or approximately equal to the 0.0075 radians design drift limit. However, for some of the scaled earthquakes, the story shears may exceed the design limit (estimated from Figure 9).

Comparison of analysis results with the design intent indicates the design approach is a practical means of proportioning a structure, which can closely correspond to the strength and drift requirements of the DBE. The design story shear is conservative due to the use of T_a instead of the actual building period T (Equation (8)). However, the design base shear may be unconservative by using steady state elliptical response assumption, which may not hold for a pulse type earthquake (Northridge) and large VE-damping. Additionally, assuming only first mode response through use of a 1.33 reduction factor (Equation (8)) and ignoring higher mode response on the design base shear is unconservative. This was particularly evident for Castaic (Figure 9), a Northridge earthquake, which exhibited higher mode response as shown by the nonuniform drift in Figure 8. Due to these uncertainties, it would appear reasonable to use T_a instead of T for determining the design base shear. Additional research is required to characterize VE-system behavior under pulse type earthquake motions and corresponding higher mode response so that a rational approach can be developed to incorporate these factors.

Analysis results also indicated column and beam moments and shear forces tended to be in-phase with frame displacements while the axial forces for these members tended to be more in-phase with the damper forces. Member axial forces were strongly influenced by the dampers because of the high K'_d/K_f stiffness ratio used in the high damping design, which results in large damper forces that must be transmitted to the frame members. The viscous forces in the steel frame members produced by the VE-dampers are described further in the experimental results. It is important to note that if global Rayleigh damping is used to model the damping provided by the VE-dampers, the out-of-phase response of the frame and members is not captured and requires correction to predict peak forces (Kasai and Fu 1995). The VE-damper fractional derivative model used in this study did capture out-of-phase member forces and was well correlated

EXPERIMENTAL METHOD

A unique methodology was developed to test a portion of the prototype VE-frame because it is currently prohibitive to test a 10-story structure at full-scale due to specimen size and limitations in laboratory testing capabilities. The test specimen was the full-scale, lower 3-story portion, of the prototype 10-story VE-frame and was subjected to large magnitude vertical and earthquake forces as illustrated in Figure 10. The key feature of the experimental program was the use of the displacement response from time-history analysis of the 10-story prototype VE-frame as the input motion to the test structure. The mass, stiffness, and damping of the full 10-story frame were incorporated into the computer model and their properties are reflected in the analytically computed displacement response. Analytically predicted frame response at the third story level was imposed to the laboratory test frame. All experiments were performed dynamically, in real-time, due to the velocity sensitive properties of the VE-material.

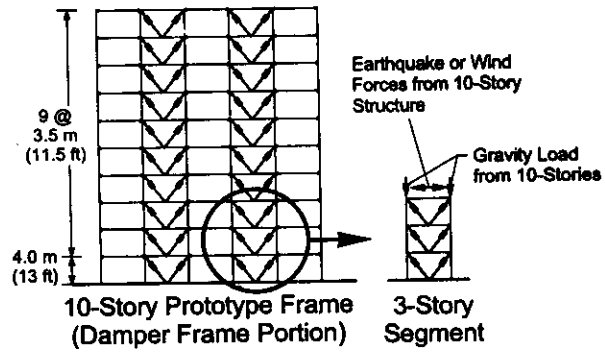

Fig. 10 Methodology for experiment

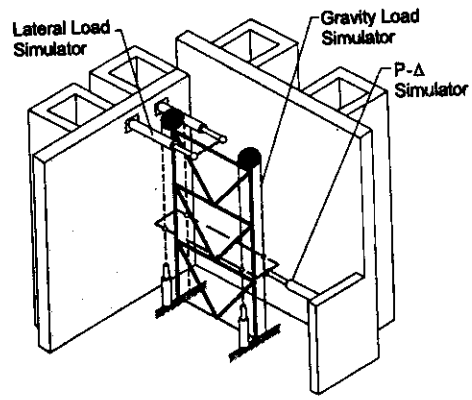

Fig. 11 Schematic of test set-up

The test set-up is shown schematically in Figure 11 and the three-story portion of the prototype building tested in the laboratory is shown in Figure 12. The experiment incorporated over 90 % of the tall reaction wall in the ATLSS Laboratory at Lehigh University, one of the largest in the North America. Cumulative axial forces from gravity loads from the complete 10-story structure were applied to the column tops of the frame test specimen by 76 mm (3 in) diameter wire ropes attached to two actuators (Figure 12a and 12b). Vertical forces up to 4.45 MN (1000 kips) develop in each column due to gravity and lateral load effects during some tests. Large earthquake loads accumulated from the 10-story structure were applied at the third story level through two additional hydraulic actuators. In general,

highly damped structures, like the VE-damped prototype frames, behave predominantly in the first mode. The first mode has a straight line deflected shape and as a result, the test structure only requires lateral force actuators at the third story location to accurately simulate the displacement response within all three lower stories. Second order or $P-\Delta$ effects were simulated with a fifth actuator, which ensures that the simulated gravity force remains vertical despite tilting of the frame (Figure 12c).

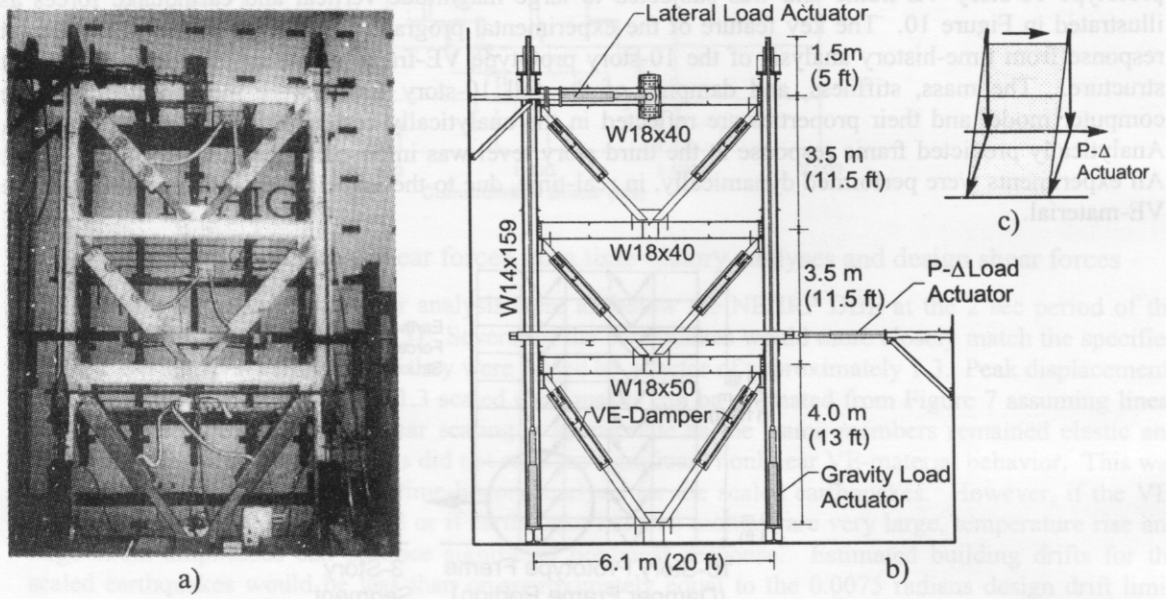

Fig. 12 Viscoelatic frame test specimen

During each test, data were acquired from 196 channels using a PC-based high-speed data acquisition system. Sensors included strain gages, position sensors, load cells. These sensors enabled measurement of both overall global frame response and local member responses. Thermocouples were inserted into the VE-material to monitor damper temperature changes. Initial damper temperatures were controlled by placing insulated enclosures around each damper. Forced air, either heated or cooled, was blown into the enclosures until the desired initial VE-material temperature was achieved.

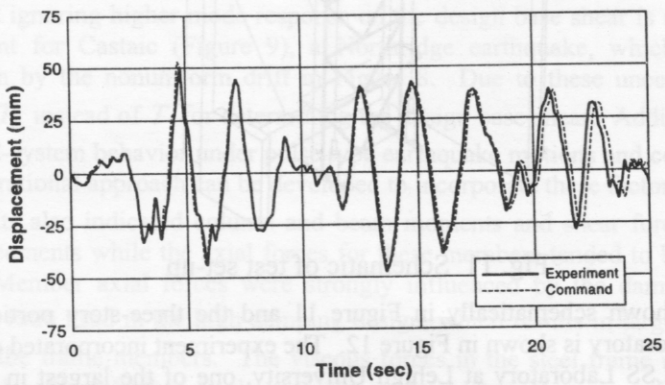

Fig. 13 Target and measured displacement at 3rd story for 1.5 x Hachinohe

Example target and measured displacement time history at the third story level is shown in Figure 13 for the Hachinohe earthquake. A comparison of the target and measured displacement response indicates

some small details of the response record is lost, the peak displacements tend to be slightly lower than the target displacement, and there is some elongation of the time scale between the actuator command and actual displacements. In general however, the displacement response was reasonably well captured. The observed differences between target and measured responses were due to physical limitations of the hydraulic and control systems for these demanding tests.

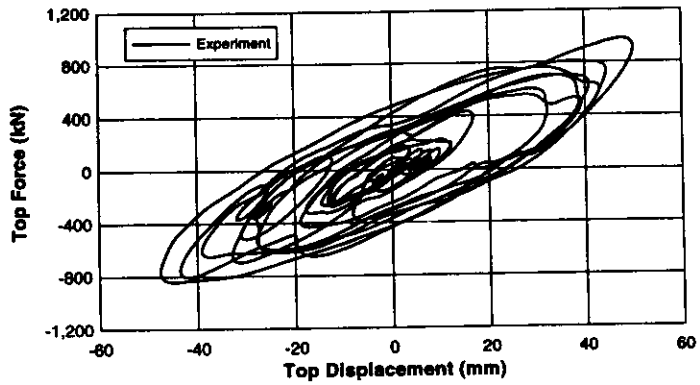

Fig. 14 Measured overall force-displacement response for 1.5 x Hachinohe

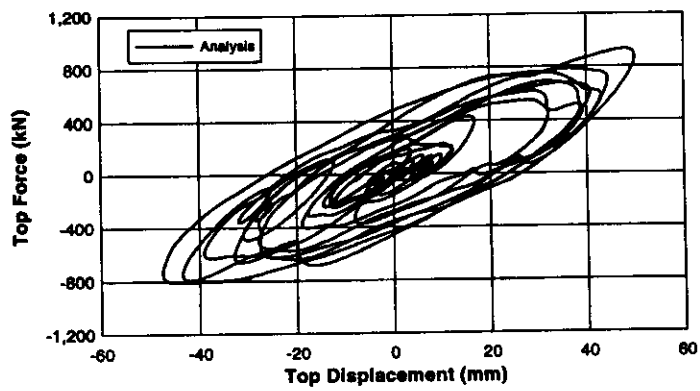

Fig. 15 Analytically predicted overall force-displacement response for 1.5 x Hachinohe

Example measured overall force-deformation response for the frame is shown in Figure 14 for the Hachinohe earthquake. Analytically predicted overall force-deformation response for the laboratory imposed motion of Hachinohe is shown in Figure 15. As shown in Figures 14 and 15, the measured and predicted responses are similar and the methodology reasonably reflects the seismic response of the prototype building. Overall responses indicated the dampers provided significant energy dissipation for all earthquakes. This energy dissipation by the dampers during the earthquakes results in temperature rise within the VE-material. Measured temperature rise in a typical second story damper is shown in Table 5 for each of the nine earthquakes. The largest observed temperature rise (3.4°C) was recorded during the Mexico City: Central de Abastos-Frigorifico earthquake. This response was 60 sec in duration and contained many significant excursions. Temperature rise in the dampers can be predicted according to Kasai et al.'s method (1993) as the total area or dissipated energy density obtained from the stress-strain loops of the damper divided by the product of specific heat and density of the VE-material (=1958.1 kPa/°C (0.284 ksi/°C) for the given VE-material). Damper temperature rise predicted according to this method is also shown in Table 5.

Table 5: Measured and Computed VE-Damper Temperatures for Each of the Nine Earthquakes Investigated

Earthquake Record	Damper Location (Story Level)	Initial Temperature (°C)	Final Temperature (°C)	Computed Temperature# (°C)
Castaic	L2	23.9	25.7	26.0
El Centro	L2	23.9	25.7	26.2
Mexico City: Frigorifico	L2	23.9	27.3	27.1
Hachinohe	L2	23.9	26.1	26.1
Oakland	L2	23.9	24.9	24.8
Mexico City: Oficina	L2	24.0	26.2	26.3
Santa Monica	L2	23.9	25.4	25.5
Taft	L2	23.9	26.1	26.7
Treasure Island	L2	23.9	24.7	24.7

According to Kasai *et al*. 1993.

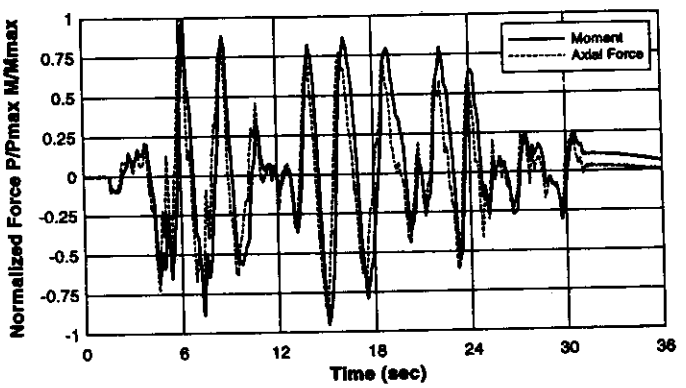

Fig. 16 Normalized measured moment and axial force in 2nd story beam during 1.5 x Hachinohe

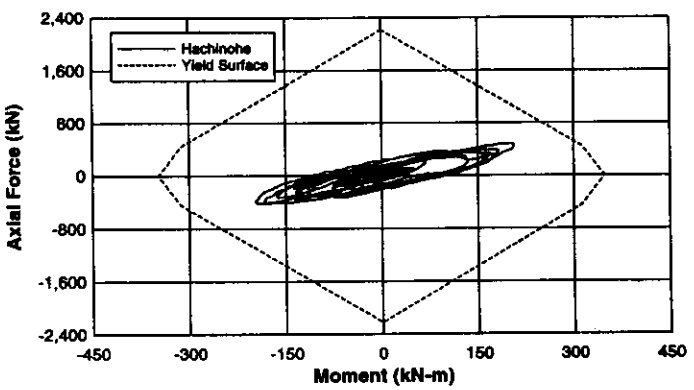

Fig. 17 Measured moment-axial force interaction in 2nd story beam during 1.5 x Hachinohe

In addition to overall frame response, data was collected which also enabled assessment of local member responses. Data and observations indicated that the frame members remained elastic during all tests with the exception of minor local yielding near connections. Measured column and beam moments (and shear forces) tended to be in-phase with frame displacement, while axial forces tended to be in-phase with the VE-damper forces. As an example, the normalized measured time-history response for moment and axial force in the second story beam are shown in Figure 16. There is a phase-lag between the axial force and moment due to a viscous force component transferred to the beam by the VE-dampers as seen in Figure 16. Maximum axial force and bending moment do not occur at the same instant of time due to the phase-lag and thus members exhibit moment-axial force interaction as shown in Figures 17. Similar types of moment-axial force interaction were also observed for the column members. The out-of-phase member forces generated by the dampers can be predicted by the author's method (Kasai and Fu 1995) and although the peak moment and axial forces do not occur at the same time, it is conservative to design these members assuming they occur simultaneously.

CONCLUSIONS

A prototype VE-frame has been designed, analyzed and tested. Design was performed using an equivalent lateral force procedure with specified high-performance design criteria which included elastic performance and small drift (< 0.0075 radians) at the reference temperature of 24°C under the California type DBE, which has a return period of about 500 years. Subsequent analysis and testing indicated the design methodology provides a practical means of designing VE-damped steel frames which can closely correspond to the strength and drift requirements of the DBE. However, for some near field pulse type earthquakes or when significant higher mode effects are present, the methodology may not be conservative. Additional research is required so that a rational approach can be developed to incorporate these factors. Following design of the prototype frame, a unique methodology was developed to enable testing of the full-scale lower three story portion of the 10-story prototype VE-damped frame subjected to significant seismic and gravity forces. Measured overall frame, member, and damper responses for the earthquake motions indicated significant energy dissipation is provided by the VE-dampers and that the steel members behaved elastically. Analytically predicted response and measured experimental response were well correlated indicating the testing methodology is reasonable. Measured moments and shear forces in frame members were in-phase with frame displacement, while the axial forces had significant out-of-phase components due to VE-damper forces. The phase lag between moment and axial force in the beams and columns results in peak forces occurring at different instances of time and an interaction between the forces. A proposed simplification would conservatively design members assuming the peaks occur simultaneously.

ACKNOWLEDGEMENTS

The tests were conducted in the Advanced Technology for Large Structural Systems Laboratory (ATLSS) at Lehigh University. The support of the 3M Company, National Science Foundation, Nippon Steel, Bethlehem Steel, and Lukens Steel is gratefully acknowledged.

REFERENCES

1. Architectural Institute of Japan (AIJ) (1990). "Ultimate Strength and Deformation Capacity of Buildings in Seismic Design," Architectural Institute of Japan, Tokyo (in Japanese).
2. Aiken, I. And Kelly, J.M. (1991). "Earthquake Simulator Testing of Two Damping Systems for Multistory Structures," Proceedings of Damping 1991 Vol. II, San Diego, CA, FCA-1-FCA-13.
3. American Institute of Steel Construction (AISC) (1993). "Manual of Steel Construction-Load and Resistance Factor Design," Second Edition, AISC, Chicago, IL.

4. American Society of Civil Engineers (ASCE) (1996). "ASCE 7-95 Minimum Design Loads for Buildings and Other Structures," ASCE, New York, NY.
5. Chang, K.C., Soong, T.T., Oh, S.T. and Lai, M.L. (1991). "Seismic Response of a 2/5 Scale Steel Structure with Added Viscoelastic Dampers," Technical Report NCEER-91-0012, State University of New York at Buffalo, NY.
6. Chang, K.C., Soong, T.T., Oh, S.T. and Lai, M.L. (1995). "Seismic Behavior of Steel Frame with Added Viscoelastic Dampers," Journal of Structural Engineering, ASCE, Vol. 121, No. 10, pp. 1418-1426.
7. Fu, Y. and Kasai, K. (1998). "Comparative Study of Frames Using Viscoelastic and Viscous Dampers," Journal of Structural Engineering, ASCE, Vol. 124, No. 5, pp. 513-522.
8. Higgins, C. and Kasai, K. (1998). "Experimental and Analytical Simulation of Along-Wind Response for a Full-Scale Viscoelastically Damped Steel Frame," Journal of Wind Engineering and Industrial Aerodynamics, Vol. 77-78, pp. 297-313.
9. Kasai, K. and Higgins, C., (1997). "Real-Time and Full-Scale Tests of a Viscoelastically Damped Steel Frame Under Large Seismic and Gravity Loads," International Conference on Behavior of Steel Structures in Seismic Areas, STESSA '97, Kyoto, Japan.
10. Kasai, K., and Fu, Y. (1995). "Seismic Analysis and Design Using Viscoelastic Dampers," A New Direction in Seismic Design, Architectural Institute of Japan, Tokyo, pp. 113-140.
11. Kasai, K., Fu, Y. and Watanabe, A. (1998). "Passive Control Systems for Seismic Damage Mitigation," Journal of Structural Engineering, ASCE, Vol. 124, No. 5, pp. 501-512.
12. Kasai, K., Munshi, J.A., Lai, M.L. and Maison, B.F. (1993). "Viscoelastic Damper Hysteretic Model: Theory, Experiment, and Application," ATC-17-1 Seminar, San Francisco, CA, pp. 521-532.
13. Kasai, K., and Popov, E. P. (1986). "A Study of Seismically Resistant Eccentrically Braced Frames," EERC Report 86-01, University of California, Berkeley, CA.
14. Maison, B.F. (1992). "PC-ANSR: A Computer Program for Nonlinear Structural Analysis," National Information Service for Earthquake Engineering.
15. Miranda, E. (1993). "Evaluation of Site Dependent Inelastic Seismic Design Spectra," Journal of Structural Engineering, ASCE, Vol. 119, No. 5, pp. 1319-1338.
16. National Earthquake Hazards Reduction Program (NEHRP) (1994). "NEHRP Recommended Provisions for Seismic Regulations for New Buildings," Building Seismic Safety Council, Washington, D.C.
17. Seed, H. B., Ugas, C., and Lysmer, J. (1976). "Site-Dependent Spectra for Earthquake-Resistant Design," Bulletin of the Seismological Society of America, Vol. 66, No. 1, pp. 221-241.